

# Characterisation and Control of Fibre Alignment during Prepreg Manufacture

C.J.Creighton<sup>†</sup>, M.P.F.Sutcliffe<sup>§</sup> and T.W.Clyne<sup>†</sup>

<sup>†</sup> *Department of Materials Science and Metallurgy  
University of Cambridge  
Pembroke Street, Cambridge, CB2 3QZ, UK*

<sup>§</sup> *Department of Engineering  
University of Cambridge  
Trumpington Street, Cambridge, CB2 1PZ, UK*

## SUMMARY:

A procedure is presented for characterization of fibre misalignment in composites. It is based on analysis of low magnification images in which the local fibre direction can be inferred from the orientation of elongated features in the image. Specimen preparation and image analysis procedures are presented and their usage is illustrated by application to a carbon fibre composite. Factors affecting the choice of certain image analysis parameters are briefly explored. It is shown that the proposed method is robust, sensitive and experimentally convenient. It is particularly well-suited to the characterisation of specimens exhibiting significant variations in fibre alignment direction over large distances, ie pronounced fibre waviness, and the potential utility of such measurements for the prediction of compressive strength is highlighted.

## 1 INTRODUCTION

A degree of fibre misalignment or waviness commonly arises during processing of long fibre composites. Characterisation of fibre alignment is an important objective in the science and technology of these materials, particularly in terms of the axial compressive strength. Most models<sup>1,2</sup> for compressive failure focus on shear failure parallel to the fibre axis, which occurs more readily with increasing misalignment between this direction and the loading axis. These apparently give fairly good quantitative agreement between prediction and measurement when applied to a range of polymer composites<sup>3-9</sup>, although there has often been considerable uncertainty surrounding the definition and measurement of the appropriate misalignment angle. The basic principles involved in prediction of this type of shear instability have also been incorporated into numerical models<sup>10-12</sup>, allowing investigation of the effects of variables such as the size and shape of the initially misoriented region.

Prediction of the compressive strength of a composite containing an arbitrary spatial distribution of fibre alignment angles is hampered by limitations in experimental characterisation of fibre alignment. The method most commonly used hitherto to establish the misalignment angle is a simple sectioning procedure<sup>13,14</sup>, involving examination of sections lying at a selected angle to the nominal fibre alignment direction. The aspect ratios exhibited by individual fibres in such sections are measured, usually with image analysis software. These values are then transformed into angular misalignments, assuming the fibres to be of

circular cross-section and hence elliptical in the viewed section. It is also possible, by noting the angle between a reference direction and the major axis of the ellipse, to obtain information about the three-dimensional orientation distribution. However, this method is extremely cumbersome and can only give information about the orientation of a relatively small number of fibres at a few locations within the material. Furthermore, any attempt to record changes in the alignment of individual fibres along their length, for example by serial sectioning<sup>15</sup> or confocal scanning laser microscopy<sup>16</sup>, renders the technique even more time-consuming. Finally, the method is inherently destructive and is unsuited to quality control requirements during monitoring of production operations.

In the present paper, a specimen preparation and image analysis procedure is presented which allows rapid acquisition of fibre alignment data characterising large regions of the material, in a form which is well suited for use in models of compressive failure.

## 2 BACKGROUND (PREPREG MANUFACTURE, LAY-UP AND CONSOLIDATION)

Prepregs are thin sheets of fibres impregnated with resin. The most frequently used method of prepreg manufacture is the film route, which is illustrated schematically in figure 1. Tows of fibre are pulled along a heated bed, where resin films are brought into contact with them on upper and lower surfaces. The thermal field is controlled so as to reduce the resin viscosity sufficiently to allow tow infiltration under the pressure applied via the consolidation rolls and to promote curing. Finally the prepreg is backed with release film for storage until required for component manufacture.

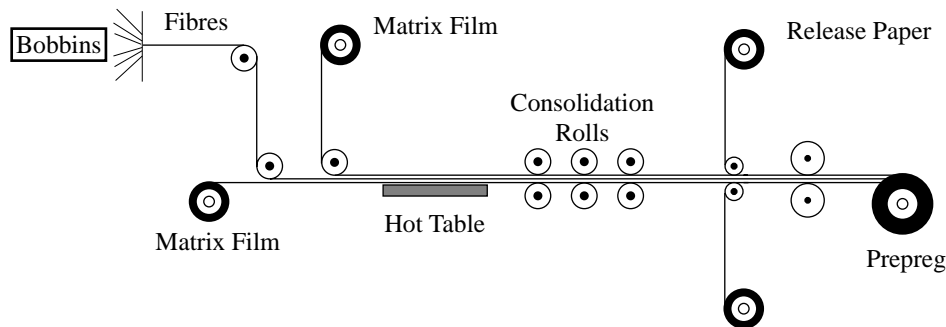


Figure 1 Schematic of the film route prepreg manufacturing procedure

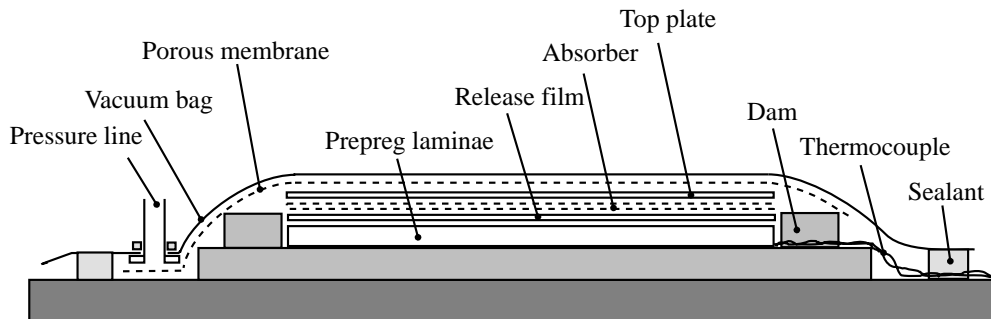


Figure 2 Composite lay-up prepared for curing

Consolidation involves the cutting and stacking of prepreg layers in a predetermined sequence of fibre orientations within a mould containing release agent and absorption layers. An upper plate is laid on top and this assembly is sealed in a vacuum bag, as shown in figure 2. The matrix resin is cured by exposure to a defined combination of temperature and pressure.

When the lay-up is heated, the constraint offered by the resin decreases as its viscosity falls. Application of pressure forces the fibres together. Therefore the temperature and pressure cycle affects, not only the fibre volume fraction and void content, but also the fibre distribution and alignment. The fibre alignment characterisation technique presented here can be applied to fully cured composite components and to prepreg material.

### 3 IMAGE ACQUISITION AND ANALYSIS

#### 3.1 Specimen Preparation

Specimens were prepared by sectioning and grinding down to 1200 grit SiC paper. This surface was then flooded with acetone and rubbed with wire wool parallel to the fibre direction, using fingertip pressure, for a period of a few minutes. This process removed some of the epoxy matrix and established good contrast between the fibre and matrix, when viewed under the optical microscope. Slight variations to this procedure may be needed for different composite systems, but in general it should not be difficult to produce suitable levels of contrast for a wide range of materials.

#### 3.2 Image Analysis Algorithm

An automated procedure is necessary in order to obtain the necessary data within acceptable time and precision constraints. The field of interest is first divided up into a number of domains,  $A_j$ . A schematic representation of this is shown in figure 3. The co-ordinates of the centroid of each domain, and its dimensions, should be specified in such a manner that a representative region is being sampled. Alternatively, localised characteristics may be obtained.

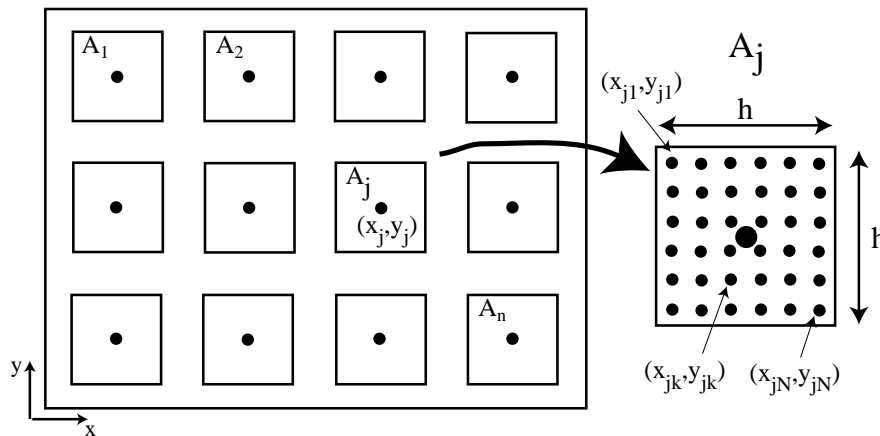


Figure 3 Schematic depiction of a set of domains ( $A_j$ , centred at  $x_j, y_j$ ) to be superimposed on the image of the composite, within which the average fibre orientation  $\phi$  is to be measured.

An image analysis algorithm is required to measure the fibre orientation angle,  $\phi$ , in a given domain. Consider the dark elongated features (which might represent fibres, or matrix between fibres, or bundles of fibres) oriented at an angle  $\phi$  to the reference (horizontal) direction in figure 4. For a pixel array inclined at an angle  $\theta$  to the horizontal, the variation in light intensity,  $I$ , with distance along the array will be as depicted schematically for the two cases shown, corresponding to  $\theta$  being close to, or significantly different from,  $\phi$ . When the array is oriented along the axis of the fibrous feature ( $\theta = \phi$ ), the minimum in light intensity corresponding to the dark feature has a width equal to the length of the fibre (or, more precisely, to that length of the fibrous structure for which the contrast in the image is

uniform). At all other orientations, the trough representing the fibrous feature is expected to be narrower than this.

An intensity variation parameter,  $\delta$ , is now defined as the average of the absolute differences between the intensity  $I_0$  at the midpoint of the linescan and the intensities within a suitable distance  $L/2$  on either side of the mid-position (i.e. for pixel numbers between  $\pm m$ ). If the intensities are sampled along the pixel array, for an array inclined at an angle  $\theta$ , the corresponding value of  $\delta$  can be obtained from

$$\delta_\theta = \frac{1}{2m+1} \sum_{i=-m}^{i=+m} |I(P_0) - I(P_i)| \quad (1)$$

where the intensities  $I(P_i)$  are sampled at  $2m+1$  points regularly spaced along the length of the pixel array. The magnitude of  $\delta_\theta$  is a measure of the extent to which the intensity varies along the direction concerned, with small values indicating little variation. The orientation of the fibrous feature corresponds to the angle  $\theta$  for which the magnitude of  $\delta_\theta$  has a minimum value.

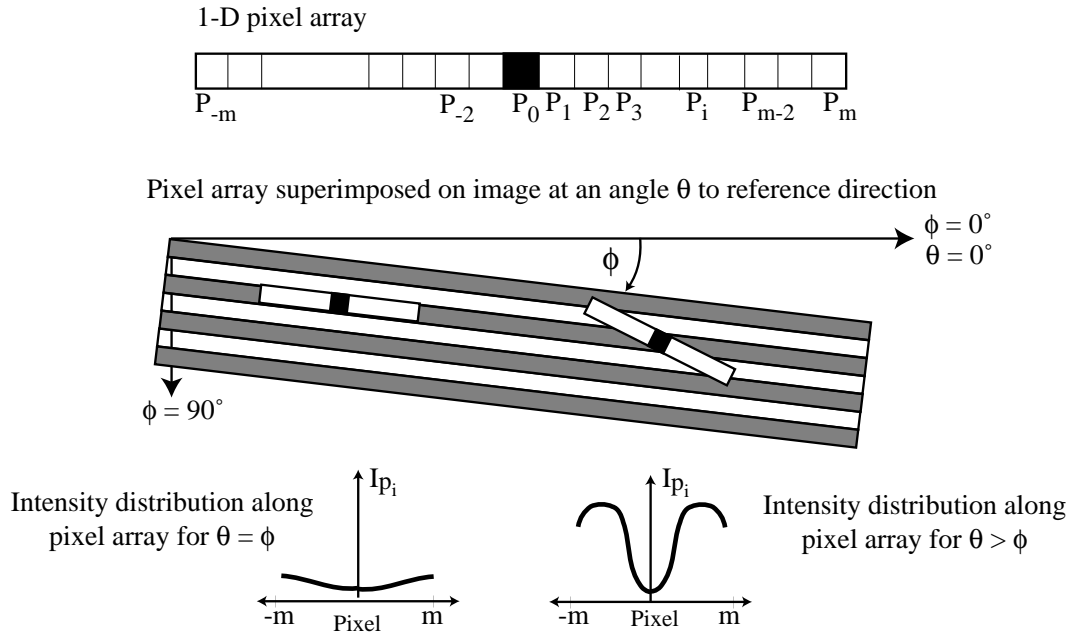


Figure 4 Schematic depiction of a 1-D array of pixels within an image, inclined at an angle  $\theta$  to the reference direction, showing typical intensity distributions along the length of the array, for two values of  $\theta$ , one of which is equal to and the other greater than the fibre misalignment angle  $\phi$ .

The above operation is carried out at a specified point, defined, as shown in Fig.1(b), by the co-ordinates  $(x_j, y_j)$ , which is the location of the centroid of the pixel array ( $P_0$ ) for all values of the orientation  $\theta$ . In order to characterize the average alignment within a domain,  $A_j$ , the operation is repeated at a series of points located within  $A_j$  - see Fig.3. These points lie on a grid,  $(x_{jk}, y_{jk})$ ,  $k=1 \rightarrow N$ , located in the vicinity of  $(x_j, y_j)$ .

$$\delta_{\theta,j} = \frac{1}{N} \sum_{k=1}^{k=N} \delta_\theta \quad (2)$$

This leads to an average value of  $\delta$ , within the domain  $A_j$ , for each of a series of angles  $\theta$  to the reference direction. A plot of  $\delta$  against  $\theta$  leads to curves of the form shown in Fig.5. The value of  $\phi$ , representative of the alignment direction within the domain, is taken as equal to the value of  $\theta$  where the minimum occurs in the curve. It can be seen from the curves in Fig.5

that the deduced value of  $\phi$  is not sensitive to the length of the array of pixels. This is discussed below in §3.3. The averaging procedure described was found to give very similar results to those from more complex autocorrelation and Fourier analysis techniques, and in fact is to be preferred to such methods since it appears to be a more robust, reliable and accurate technique for this application.

In summary, the following sequence of operations was carried out in order to implement the analysis:

- A photograph of the microstructure was scanned at a suitable size and resolution (or a digital image could be obtained directly). In the current work, the image was typically of a field with linear dimensions of a few mm, although larger areas can be examined by stitching together several images. The magnification used was typically such that each pixel was a square of side about  $3\ \mu\text{m}$ . This leads to approximately 500,000 pixels per image, each of which is assigned one of 256 grey scale levels.
- A set of square domains,  $A_j$ , was defined in terms of the co-ordinates of the centroid,  $(x_j, y_j)$ , the length of the side,  $h$ , and the number of points,  $N$ , within the domain at which analysis is to be carried out. In the present work, this set of points formed a square grid,  $(x_{jk}, y_{jk})$ ,  $k=1\rightarrow N$ , with  $N$  equal to the number of scanned pixels in the domain.
- The grid of points within each domain was rotated to an angle  $\theta$  relative to the reference direction. The light intensity along the 1-D pixel arrays produced in this way is calculated from the original pixel array of the scanned image using a cubic interpolation procedure. The value of  $\delta$  corresponding to this angle  $\theta$  for a single pixel array is obtained using eqn.(1) and the average value of  $\delta$  for the set of pixel arrays lying at this angle,  $\delta_{\theta j}$ , is obtained using eqn.(2). Padding of the data is used at the edges of the domain, taking the intensities outside the domain equal to the values at the nearest pixel inside the domain.
- By rotating the grid through a series of  $\theta$  values and repeating the operation, a plot of  $\delta_{\theta j}$  against  $\theta$  was generated and the value of  $\theta$  corresponding to the minimum in this plot was taken as the  $\phi$  value characteristic of the domain.

This procedure was then repeated for each domain in the field. Using the parameter values outlined above, the complete operation typically takes about 3 hours on a standard workstation, for a set of domains covering a typical image field.

### 3.3 Precision and Sensitivity

Two parameters central to the analysis are chosen arbitrarily. These are the length of the pixel array,  $L$ , and the length of the side of the domains,  $h$ . The effect of varying the value of  $L$  was shown in figure 5. It can be seen that the deduced value of  $\phi$  ( $\sim -1.5^\circ$  in this case) is not sensitive to the chosen value of  $L$ . As long as  $L$  is not much less than the characteristic length of features in the image ( $\sim 100\ \mu\text{m}$  in this case), the outcome should be insensitive to the value chosen. It may be noted that there are some anomalous data around  $\theta=0^\circ$ , particularly for the shortest value of  $L$  ( $32\ \mu\text{m}$ ). This is a consequence of certain characteristics of the cubic interpolation procedure. Errors in the deduced value of  $\phi$  due to this effect can be avoided by ensuring that the pixel orientation in the scanned image does not coincide with the fibre orientation.

The effect of domain size can be seen in figure 6, which shows the dependence of the estimated fibre misalignment angle  $\phi$  on the domain side length  $h$ . For very small values of  $h$

(<200  $\mu\text{m}$ ), there are insufficient data to extract a reliable estimate of  $\phi$ . At intermediate values (200  $\mu\text{m} < h < 400 \mu\text{m}$ ), there is a region where  $\phi$  changes little with domain size. For larger values than this, averaging is now being done over a region within which  $\phi$  changes significantly with position, so that the deduced value starts to vary again. Hence the spatial resolution of the method is about 200  $\mu\text{m}$ . This is more than adequate to capture typical variations in fibre misalignment angle with position.

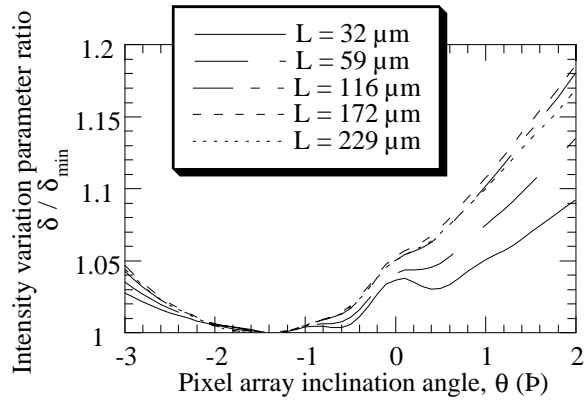


Figure 5 Image analysis data obtained from a prepregged sheet material. Plots are shown of the measured value of the intensity variation parameter,  $\delta$ , as a ratio to the minimum value obtained, as a function of the inclination,  $\theta$ , of the pixel array to the reference direction. The curves correspond to different values of  $L$ , the length of the pixel array

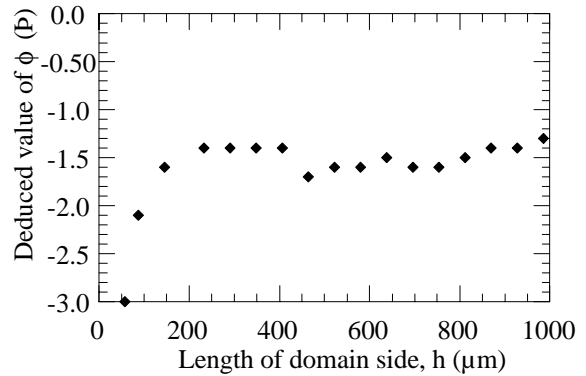


Figure 6 Image analysis data obtained from the prepregged sheet, showing the effect of altering the length of the domain side on the deduced value of the average fibre misalignment angle,  $\phi$ , within the domain.

#### 4 RESULTS

A typical result is presented in figure 7, which shows (a) an image of the free surface of a consolidated sheet, about 20 mm  $\times$  5 mm, and (b) a corresponding contour map showing how the average misalignment angle varies with position. This map was obtained by measuring the value of  $\phi$  in about 200 domains, centred on the regular grid of points superimposed on the image. In this particular example, a noticeably wavy region is apparent in the micrograph near the top edge, about one third of the way along. This is apparent in the contour map as a region in which  $\phi$  varies between about  $\pm 5^\circ$ . This is the type of information needed for comprehensive prediction of the compressive strength of such material, using models which take into account the size, shape and average fibre inclination of misaligned regions.

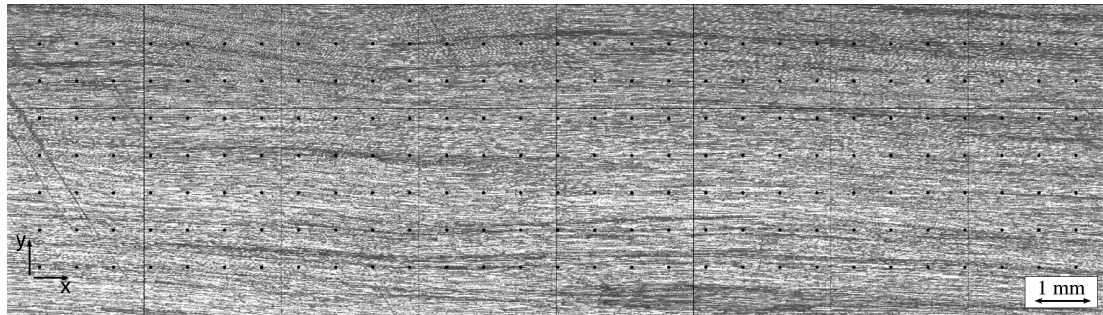


Figure 7(a)

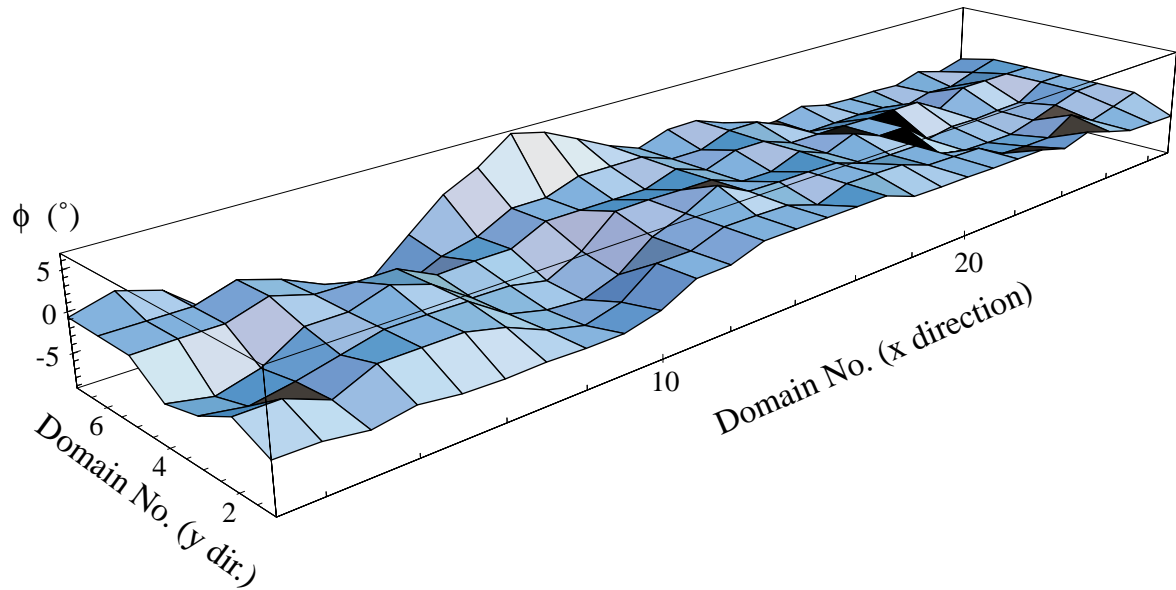


Figure 7 (b)

Figure 7 (a) Optical micrograph showing the free surface of prepregged sheet material, with the centroid of each measurement domain marked by a black dot, and (b) corresponding contour map of measured average misalignment angle within each domain, with each grid intersection point corresponding to one of the black dots in the micrograph.

## 5 CONCLUSIONS

- a) A new technique is presented for measurement of fibre misalignment distributions within a composite material. It is based on image analysis of low magnification micrographs in which the local fibre alignment direction is indicated by the orientation of elongated light and dark features.
- b) Specimen preparation and microscopy procedures have been described which led to production of suitable images when applied to two types of carbon fibre composite. Similar techniques are expected to be applicable to a wide range of composite types. A relatively simple image processing algorithm has been outlined which allows the local fibre alignment direction to be measured on a digitised image. The method is well-suited to the characterisation of large volumes of material without the procedure becoming unduly time-consuming, either experimentally or in terms of computing time.
- c) Two arbitrarily chosen parameters are involved in the image analysis procedure. These are the length of the pixel array used to determine the fibre orientation and the size of the domain over which the measured fibre alignment is averaged. The effects of varying these parameters have been briefly investigated.
- d) The results obtained are insensitive to the pixel array length, provided it is greater than a characteristic feature length. This is expected to be related to fibre diameter. In the present work, with a fibre diameter of about  $7 \mu\text{m}$ , the feature length was found to be of the order of  $100 \mu\text{m}$ .

- e) In the present work, the domains used have all been square. Very small domains tend to lead to unreliable results, particularly if the sides are shorter than the characteristic feature length. In the present work, a domain side length of between about 200  $\mu\text{m}$  and 400  $\mu\text{m}$  was found to give consistent results. The procedures are reliable for larger domains, but the measured average misalignment angle tended to fluctuate as a result of significant variations in local fibre alignment within the domain.
- f) The proposed method is particularly well-suited to composite specimens exhibiting long range spatial variations in fibre alignment (waviness) and it has been shown how contour maps can be constructed to present misalignment data obtained over large areas of material.

### ACKNOWLEDGEMENTS

This work was carried out as part of a studentship supported by the EPSRC, within a programme involving Hexcel Composites, British Aerospace, DERA and Neptco. The authors are grateful for useful discussions with P.M.McClellan and S.O'Meara, of Neptco, with Dr.J.Ball, of British Aerospace, and with Prof.N.A.Fleck, of Cambridge University.

### REFERENCES

1. A. S. Argon, *Fracture of Composites*, Vol. 1, Academic Press, New York, (1972).
2. B. Budiansky and N. A. Fleck, *Compressive Failure of Fibre Composites*, J. Mech. Phys. Sol., **41** (1993), pp. 183-211.
3. M. R. Piggott and P. Wilde, *Compressive Strength of Aligned Steel Reinforced Epoxy Resin*, J. Mat. Sci., **15** (1980), pp. 2811-2815.
4. M. R. Piggott and B. Harris, *Compression Strength of Carbon, Glass and Kevlar 49 Fibre Reinforced Polyester Resins*, J. Mat. Sci., **15** (1980), pp. 2523-2538.
5. M. R. Wisnom, *The Effect of Fibre Misalignment on the Compressive Strength of Unidirectional Carbon Fibre / Epoxy*, Composites, **21** (1990), pp. 403-407.
6. A. L. Highsmith, J. J. Davis and K. L. E. Helms, *The Influence of Fiber Waviness on the Compressive Behavior of Unidirectional Continuous Fiber Composites*, in *Composite Materials, Testing and Design, ASTM STP 1120*, G. C. Grimes (Ed.), Vol. 1120, ASTM, Philadelphia, (1992), pp. 20-36.
7. P. M. Jelf and N. A. Fleck, *Compression Failure Mechanisms in Unidirectional Composites*, J. Comp. Mats., **26** (1992), pp. 2706-2726.
8. J. G. Häberle and F. L. Matthews, *An Improved Technique for Compression Testing of Fibre-Reinforced Plastics; Development and Results*, Composites, **25(5)** (1994), pp. 358-371.
9. M. R. Piggott, *The Effect of Fibre Waviness on the Mechanical Properties of Unidirectional Fibre Composites - A Review*, Comp. Sci. Tech, **53** (1995), pp. 201-205.

10. M. P. F. Sutcliffe and N. A. Fleck, *Effect of Geometry on Compressive Failure of Notched Composites*, Int. J. Fracture, **59** (1993), pp. 115-132.
11. W. S. Slaughter and N. A. Fleck, *Microbuckling of Fiber Composites with Random Initial Fiber Waviness*, J. Mech. Phys. Solids., **42(11)** (1994), pp. 1743-1766.
12. N. A. Fleck and J. Y. Shu, *Microbuckle Initiation in Fibre Composites: a Finite Element Study.*, J. Mech. Phys. Solids, **43** (1995), pp. 1887-1918.
13. M. Vincent and J. F. Agassant, *Experimental Study and Calculations of Short Glass Fiber Orientation in a Center Gated Molded Disk*, Polymer Composites, **7** (1986), pp. 76-83.
14. S. W. Yurgartis, *Measurement of Small Angle Fiber Misalignments in Continuous Fiber Composites.*, Comp. Sci. and Tech., **30** (1987), pp. 279-293.
15. J. R. Davis, *Compressive Strength of Fibre Reinforced Composites*, in *Composite Reliability ASTM STP 580*, ASTM, Philadelphia, (1975), pp. 364-377.
16. A. R. Clarke, G. Archenhold and N. C. Davidson, *A Novel Technique For Determining The 3D Spatial Distribution Of Glass Fibres In Polymer Composites*, Comp. Sci. Tech., **55** (1995), pp. 75-91.